Published in final edited form as:
Cell Rep. 2014 December 11; 9(5): 1661–1672. doi:10.1016/j.celrep.2014.11.015.

Human Slack potassium channel mutations increase positive cooperativity between individual channels

Grace E. Kim[#1,2], **Jack Kronengold**[#1], **Giulia Barcia**[3], **Imran H. Quraishi**[4], **Hilary C. Martin**[5], **Edward Blair**[6], **Jenny C. Taylor**[7], **Olivier Dulac**[3], **Laurence Colleaux**[8], **Rima Nabbout**[#3], and **Leonard K. Kaczmarek**[#1,2]

[1]Department of Pharmacology, Neurology, Yale University, New Haven, CT, 06520, USA

[2]Department of Cellular and Molecular Physiology, Neurology, Yale University, New Haven, CT, 06520, USA

[3]Department of Pediatric Neurology, Centre de Reference Epilepsies Rares, Hôpital Necker Enfants Malades, Assistance Publique-Hôpitaux de Paris, 75015 Paris, France

[4]Department of Comprehensive Epilepsy Center, Neurology, Yale University, New Haven, CT, 06520, USA

[5]Wellcome Trust Centre for Human Genetics, University of Oxford, Oxford OX3 7BN, UK

[6]Oxford University Hospitals Trust, Oxford OX3 9DU, UK

[7]Oxford Biomedical Research Centre, Wellcome Trust Centre for Human Genetics, University of Oxford, Oxford OX3 7BN, UK

[8]INSERM U781, Université Paris Descartes, Sorbonne Paris Cité, Institut Imagine, Hôpital Necker–Enfants Malades, 75015 Paris, France

[#] These authors contributed equally to this work.

Summary

Disease-causing mutations in ion channels generally alter intrinsic gating properties such as activation, inactivation or voltage-dependence. We examined nine different mutations of the KCNT1 (Slack) Na^+-activated K^+ channel that give rise to three distinct forms of epilepsy. All produced many fold-increases in current amplitude over that of the wild type channel. This could

Send correspondence to: Leonard K. Kaczmarek Dept. of Pharmacology School of Medicine 333 Cedar Street P.O Box 208066 New Haven, CT 06520 USA Tel: 203-785-4500 Fax: 203-785-5494 leonard.kaczmarek@yale.edu.

Competing Interests The authors declare no conflict of interest.

Author Contributions GEK designed and performed whole-oocyte electrophysiological and Western blot experiments; JK designed and performed single channel electrophysiological experiments; GB and HCM performed mutational analysis of patients' DNA samples; IHQ performed electrophysiological experiments; LC performed mutagenesis experiments; EB, JCT, OD and RN supervised clinical portions of the study; LKK supervised the electrophysiological experiments; GEK, JK, RN and LKK jointly wrote the manuscript.

not be accounted for by increases in the intrinsic open probability of individual channels. Rather, greatly increased opening was a consequence of cooperative interactions between multiple channels in a patch. The degree of cooperative gating was much greater for all of the mutant channels than for the wild type channel, and could explain increases in current even in a mutant with reduced unitary conductance. We also found that the same mutation gives rise to different forms of epilepsy in different individuals. Our findings indicate that a major consequence of the mutations is to alter channel-channel interactions.

Keywords

epileptic encephalopathy; *KCNT1*; malignant migrating partial seizures of infancy; autosomal dominant nocturnal frontal lobe epilepsy; Ohtahara syndrome; Slack channel

Introduction

The *KCNT1* gene encodes the Na^+-activated K^+ channel Slack (also known as Slo2.2). Mutations in *KCNT1* have been found in three different epilepsy syndromes (Barcia et al., 2012; Heron et al., 2012; Ishii et al., 2013; Martin et al., 2014): migrating malignant partial seizures in infancy (MMPSI) (Barcia et al., 2012; Ishii et al., 2013), autosomal dominant nocturnal frontal lobe epilepsy (ADNFLE) (Heron et al., 2012) and Ohtahara syndrome (OS) (Martin et al., 2014). In each of these cases, the patients with *KCNT1* mutations have a very high occurrence of severe mental and intellectual disability. When some of the known mutations were expressed in *Xenopus* oocytes, all mutations generated currents greater than those obtained with wild type Slack channels (Barcia et al., 2012; Martin et al., 2014; Milligan et al., 2014). While two mutations that produce MMPSI result in a 2-3-fold increase in current that mimics the activating effects of protein kinase C phosphorylation of the channel (Barcia et al., 2012), a mutation that produces OS showed a much greater increase in current (Martin et al., 2014), suggesting that other mechanisms must be involved. No change in sensitivity of the mutant channels to Na^+ ions has been found (Barcia et al., 2012). Thus it remains unknown if yet another mechanism contributes to the change in channel activity, or if the mutants share any common mechanisms for increased current.

We have now expressed nine of the previously published mutations in the Slack channel and have characterized their macroscopic currents, levels of protein expression and gating behavior at the single channel level. These nine mutations account for 27 out of the 31 epilepsy cases attributed to *KCNT1* mutations. We have found that the mutations cause minimal changes in the gating of individual ion channels, but greatly increase the cooperativity in channel gating that is detected in clusters of multiple channels.

Results

Clinical characteristics of patients with *KCNT1* mutations

The clinical characteristics of the 16 patients (10 with MMPSI, 5 with ADNFLE, and 1 with OS) are summarized in Table 1. Pharmacoresistance and acquired microcephaly were common to all MMPSI patients, although epilepsy onset ranged from 1 day of life to 2.5

months. They also developed a severe motor and cognitive delay. Among the ADNFLE patients, Patient 10 in particular presented with a severe form, with first seizure onset at 3 years with nocturnal hypermotor seizures. Seizures remain pharmacoresistant, and still frequent to date (23 yr). Four mutations from families with ADNFLE (Heron et al., 2012) were also included in our analysis. Some members of these families had a more severe phenotype that deviated from classical ADNFLE: earlier seizure onset with more pharmacoresistant epilepsy that led to intellectual disability and various psychiatric disorders (Table 1). Patient 16 had OS that presented at day 1 with spasms and focal seizures, and a burst suppression pattern on EEG, resulting in profound developmental delay (Martin et al 2014).

Three new patients, 2 with MMPSI and 1 with ADNFLE, were analyzed in this study. Both MMPSI patients had mutations considered as deleterious, inducing a change in a conserved amino acid (c.2008G>A, hA934T in Patient 6 and c.1193G>A, hR398Q in Patient 11). The same hA934T mutation was also found in multiple, unrelated MMPSI patients (Barcia et al., 2012), and the hR398Q mutation in a family with ADNFLE (Heron et al., 2012). Similarly, the mutation c.862G>A, hG288S, previously found in two MMPSI patients (Ishii et al., 2013), was also present in Patient 10, an ADNFLE patient.

KCNT1 point mutations lead to increased channel activity, with minor changes in protein expression

We have previously characterized two KCNT1 or Slack mutant channels, hR428Q and hA934T, which correspond to R409Q and A913T respectively in the rat, using two-electrode voltage clamping (Barcia et al., 2012). All the mutants listed in Table 1 and Figure 1A were generated likewise using the rat clone, which shares 92% sequence homology to the human clone, and are referred to using the rat numbering system here within. Channels were studied in *Xenopus laevis* oocytes, because its controlled expression system allowed us to make cross-mutation comparisons of channel expression. Current amplitude for wild type (WT) Slack increases slowly over 4 or more days after injection (Fig. 1B,C). When peak current amplitude was compared at the physiological membrane potential of +20 mV, all mutants had significantly greater currents than those of WT Slack. The fold-increase in channel activity had a wide range, and for some mutants (e.g. R455H), currents were already too large to quantify without saturation of the clamp amplifier 2 days after cRNA injection (Fig. 1B). For this reason, peak currents of WT Slack and the mutants were measured 1, 2 or 4 days after injection (Fig. 1B,C). We found no correlation between the fold-increase in channel activity and the type of epilepsy. This finding is consistent with the fact that some mutations, like mutations R379Q or G269S (Table 1, Fig. 1A), is found in both MMPSI and ADNFLE patients.

To determine if the increases in peak current amplitude resulted from increases in channel protein expression, we compared Slack protein abundance in membrane fractions by immunoblotting with an antibody that recognizes the N-terminus of the channel (Bhattacharjee and Kaczmarek, 2002). Use of this antibody ensured that the C-terminal mutants would not alter antibody recognition of the protein. Oocytes were homogenized after the completion of each voltage-clamp. Densitometry of Slack bands, when normalized

to the loading control Na^+/K^+ ATPase, revealed that changes in channel abundance were very minor, bearing no correlation to the increase in current (Fig. 2A). Only for the mutations A945T and G269S were levels of protein increased by approximately two-fold, levels that do not explain the greater than 13-fold increases in current (Fig. 1C and Martin et al., 2014). Overall, changes in levels of Slack protein failed to correlate with the increases in channel activity for any of the three types of epilepsy.

A subset of Slack mutants are left-shifted in their voltage dependence

Slack channels are voltage-dependent, with increasing open probability at positive potentials (Joiner et al., 1998; Yuan et al., 2003). A leftward shift in voltage-dependence can therefore increase currents at membrane potentials closer to neuronal resting potentials. We compared voltage-dependence for each of the mutants with that of WT Slack, and found that the majority of the mutants for MMPSI and ADNLFE had current-voltage relations identical to those of the WT channel (Fig. 2C,D). Comparing normalized voltage clamp traces of the MMPSI R455H and ADNFLE R907C mutants with those of the WT, however, revealed that both mutants showed a significant increase in channel activation at depolarized membrane potentials (Fig. 2B,C,D). While this change in voltage-dependence may contribute to the observed increases in current, the degree to which this mechanism alone can enhance current (20-30% at +20 mV) was not sufficient to explain the much larger increases in overall macroscopic current for these mutants.

Wild type Slack channels have both low and high opening probability patterns

To compare further the characteristics of the WT and mutant Slack channels, we carried out on-cell patch recordings from channels expressed in *Xenopus* oocytes. When patching from oocytes one routinely observes a high degree of non-uniformity in channel number. Some membrane patches contain no channels, whereas other nearby patches are of a “hot spot” containing variable numbers of channels. Figure 3 shows recordings at −80 mV from representative patches containing apparently different numbers of WT Slack channels. Despite identical experimental conditions, we found that there were two patterns of channel activity, depending on whether the patches contained few (1-3) or higher (4 or more) number of channels (1-3 channels).

Figure 3A shows a typical recording at −80 mV in which predominantly only one open channel can be detected, with rare simultaneous openings of two channels. As described previously, the channels are closed most of the time with frequent openings to subconductance (SC) states (Brown et al., 2010). We have termed such low open probability patches “low N” patches, and this recording is representative of all eight patches we recorded containing WT Slack channels in which only one opening predominates. The corresponding all-points amplitude histogram derived from prolonged (2 min) recording of currents quantifies the low open probability of the channel (Fig. 3B). Given that there are likely to be at least two channels in this patch, the size of the peak corresponding to the single channel opening level, O1, overestimates the true single channel open probability. Nevertheless, the amplitude of the O1 peak allows one to calculate the expected binomial distribution for multiple channels. If the channels are identical to those in a low N patch, and gate independently, then the probability that *k* channels are open out of a total of *N* should

follow a binomial distribution. Figure 3C shows such a calculated distribution for a patch containing six channels.

Figure 3D shows a patch, in which simultaneous openings of up to 6 Slack channels could be seen. We have termed such patches “high N” patches, and this recording is representative of 5 such recordings where four or more simultaneous openings were detected. The unitary conductances are identical to those seen in the low N patches. Inspection of the all-points histogram for this patch (Fig. 3E), however, shows that the channel open probability does not reflect what one would expect to see based on low N patches. A comparison of the observed distribution of channel openings (Fig.3E) to that expected from the binomial distribution of six independently gating low N channels (Fig. 3C) shows a marked increase in open time and multiple simultaneous openings in the high N patch.

We reasoned that the proximity of neighboring clustered channels in a high N patch might result in cooperative, or coupled gating, and deviate from independent channel behavior. Using the single channel open probability (*P*o) obtained from the low N all points histogram (Fig. 3B), we calculated the ratio of the observed *P*o at each level *k*, $P(k)_{obs}$, to the predicted distribution obtained from the binomial distribution, *P(k)binomial*. This is plotted in Figure 3F for the first three levels of channel opening. If channel behaviors are the same in both types of patches, $P(k)_{obs}/P(k)binomial$ should be ~1 regardless of the number of channels present. The results show, however, that $P(k)_{obs}/P(k)binomial$ increases with increasing *k*, suggesting a positive deviation from the binomial (Ding and Sachs, 2002).

Positive cooperativity is increased in the G269S Slack channel

The G269S Slack (hG288S) mutation has been found in both MMPSI and ADNFLE patients. Computational modeling of this mutation occurring in the S5 transmembrane domain has suggested that the introduction of a Serine residue results in structural changes in the pore forming region, which might lead to “impaired” channel function (Ishii, et al 2013). Given the nearly 10-fold increase in macroscopic current of the G269S mutation (Fig. 1B,C), we were surprised that the unitary conductance of the channel was ~80 pS, less than one half that of WT Slack channels (~180 pS) (Chen et al., 2009) (Fig. 3G,H).

As with the WT channels, we identified both low and high N on-cell patches of G269S channels. Figure 3G shows a trace with one channel predominantly open and rare simultaneous openings of a second channel. The all-points amplitude histogram in Figure 3H reflects the reduced unitary conductance and the fact that, like its WT counterpart, the channel is predominantly in the closed state. As a test of independence we constructed a binomial distribution, based on the probability of one channel opening (O1) in the Low N patch (Fig. 3H), to calculate the expected distribution for 4 independently gating G269S channels (Fig. 3I).

In sharp contrast to this prediction, recordings from a patch containing four G269S channels reveal multiple simultaneous openings, with very rare closings of all four channels (Fig. 3J). Despite the fact that the predominant peak in the all-points histogram is for the simultaneous opening of all four channels, no opening of more than four channels were ever detected, indicating that only four functional channels were present in this patch (Fig. 3K). The

reduced unitary conductance observed in the low N patches was, however, unchanged in the high N patches. This striking deviation in the experimental data from that predicted by the binomial distribution suggests that cooperative gating of clusters of G269S channels increases their overall activity.

To quantify the difference in cooperativity between the G269S channel and WT Slack channels, we plotted a Cooperativity Ratio; the ratio of the observed open probability at each level for G269S in high N patches by the mean observed open probabilities for WT Slack in high N patches (n =4) (Fig. 3D). If the degree of cooperativity were similar in both the mutant and WT channels in high N patches, this ratio should be ~1 for each level of channel opening. Figure 3L shows, however, that there is an increase in the cooperativity ratio as the number of open channels increases, reflecting a dramatic increase in positive cooperativity for G269S.

Positive cooperativity is increased in all the other Slack mutants

We carried out similar analyses for all the other mutations described in Table 1. All mutations other than G269S had unitary conductances in both low N and high N patches that were indistinguishable from those of WT Slack channels (n = 25 low N patches, n=13 high N patches). In all cases we found that the cooperativity ratio was increased over that in WT Slack channels. We provide figures of the data for 2 mutations in particular, the MMPSI R455H mutation and the OS A945T mutation, which are located in the RCK1 and RCK2 domains of the C-terminus, respectively (Fig. 1A).

In one of four low N patches for the R455H channel, we recorded the activity of an apparently true single channel (Fig. 4A). The open probability of this channel is markedly increased over that in WT or G269S Slack, as evident by the relative size of the O1 peak in its amplitude histogram (Fig. 4B) when compared to those in Figures 3B or 4B. As a result of this increased open probability, the predicted peak of the amplitude distribution for five independent channels is no longer at the closed state (Fig. 4C). Recordings from a patch containing five R455H channels, however, show that the distribution is shifted to the right over the predicted distribution (Fig. 4D,E) and that the cooperativity is greater than that of WT Slack channels (Fig. 4F), although by a smaller margin than the other mutations. This increased positive cooperativity was observed for all three high N R455H patches.

Finally, for the A945T mutation, channel activity in low N patches was low (n = 5, Fig. 4G,H). As was also found for some other Slack mutants (R409Q, A913T (Barcia et al., 2012)), subconductance states were absent or severely suppressed in the A945T mutant. The observed distribution of openings in a patch containing six channels, in which openings to a seventh level were never observed (Fig. 4J,K), is substantially right-shifted over that which is predicted by the binomial distribution for independently gating low N channels (Fig. 4I). In sharp contrast to the prediction, simultaneous closing of all channels in three high N patches of A945T channels was observed only very rarely. As a result, positive cooperativity is very much greater in the A945T mutant than in WT Slack channels (Fig. 4L).

Discussion

Including the three new patients reported here, 31 epilepsy patients have now been shown to carry a *KCNT1* mutation (Barcia et al., 2012; Epi et al., 2013; Heron et al., 2012; Ishii et al., 2013; Martin et al., 2014; McTague et al., 2013; Vanderver et al., 2014). Though the manifestation of seizures differs among these patients, the occurrence of intellectual disability is notably high. We observed an increase in channel activity for all nine mutants examined in our study, confirming previous studies (Barcia et al., 2012; Martin et al., 2014; Milligan et al., 2014) and documenting this for novel mutations hG288S and hR474H (rG269S and rR455H, respectively). We made the unexpected observation that WT Slack channels show positive cooperative gating, where gating of multiple channels deviates significantly from that predicted by the behavior of independent single channels. Moreover, each mutant channel had substantially greater cooperativity than the WT channel. Other non disease-associated mutations in the C-terminus, introduced for structure-function studies, display no gain-of-function (Barcia et al., 2012; Zhang et al., 2010). Thus, our observations provide a likely explanation for why the mutant channels produce greatly enhanced currents, revealing a novel pathophysiological mechanism that may be at work in affected epilepsy patients. It is probable that the enhanced cooperativity is an intrinsic property of these mutations and will be detected in human neurons bearing these mutations. Definitive proof of this for Slack channels, however, may have to await studies on human tissue or, potentially on animal models of the Slack-associated diseases.

In our studies, the amplitude histograms for “low N” patches were dominated by a single peak corresponding to the closed state, with only very rare simultaneous openings of more than one channel. As a result, in many cases it was not possible to be certain of the exact number of channels in the patch. Because single channel open probabilities were calculated from such low N patches, this method could have only overestimated the true single channel open probability, and the calculated binomial distribution for openings for multiple independent channels. In contrast, the number of channels in high N patches could be ascertained with greater confidence because of the increased opening probability together with the complete absence of openings above a fixed number of channels. In all cases we found that open probability was greatly enhanced in the high N patches, despite the fact that such patches could in theory contain, in addition to coupled channels, non-coupled channels that would dilute the degree of the cooperativity. Thus our calculations are, of necessity, underestimates of the true degree of cooperativity.

Cooperative gating was particularly striking for the MMPSI- and ADNFLE-associated G269S (hG288S) mutation in the S5 segment of Slack. A recent study using computational *in silico* modeling suggested this mutation could impair channel function by introducing a new hydrogen bond that would alter the structure of the inner surface of the pore region (Ishii, et al 2013). The finding that the unitary conductance of the G269S channel is reduced (~80 pS) is consistent with decreased throughput of potassium ions through the pore. Nevertheless, strongly augmented cooperative gating in this mutant increased macroscopic currents by ~10 fold over those of WT Slack.

Our finding of 1-3 channels in low open probability patches, and 4 or more in the high activity patches, is consistent with what others have seen for cooperatively gating channels (Molina et al., 2006; Navedo et al., 2010). The co-localized spatial distribution or "clustering" of ion channels in specific cellular regions of neurons has been shown to be a necessary determinant of neuronal excitability (Vacher and Trimmer, 2012). In addition, a functional coupling of channels in a physical cluster, where the gating of one channel is directly coupled to the gating of neighboring channels, has been observed in a number of ion channel types at the single-channel level, including KcsA (Molina et al., 2006), Na^+ (Naundorf et al., 2006), Ca^{2+} (Navedo et al., 2010), Kir 4.1 (Horio et al., 1997), AMPA (Vaithianathan et al., 2005), HCN (Dekker and Yellen, 2006), $P2X_2$ (Ding and Sachs, 2002), CFTR (Krouse and Wine, 2001) and ryanodine receptors (Laver et al., 2004; Marx et al., 2001; Marx et al., 1998). A recent study reported increased positive cooperative gating in L-type Ca^{2+} channels during hypertension and Timothy Syndrome (Navedo et al., 2010). To our knowledge, that a cohort of seemingly unrelated mutations in one channel will all increase channel gating behavior is a novel observation.

Our results also indicate that the degree to which KCNT1 mutations increase current amplitude in an expression system cannot readily be correlated with the clinical phenotype. MMPSI, with its signature early onset and pharmacoresistance, is more detrimental than ADNFLE. Across MMPSI mutants, increases in current over WT Slack ranged from 3 to 22 fold. Consistent with earlier suggestions (Milligan et al., 2014), increases for ADNFLE mutations were slightly smaller, ranging from 1.5 to 11 fold. Nevertheless a small (3 fold) increase in Slack channel activity can lead to MMPSI (rR409Q), while a greater increase (11 fold) can produce the less severe condition of ADNFLE (rY775I).

Earlier studies found distinct *de novo* or germ line mutations in MMPSI, ADNFLE or OS patients, and in some cases, the same mutation was found in multiple patients with the same diagnosis (Barcia et al., 2012; Heron et al., 2012; Ishii et al., 2013). This raised the possibility that there is a correlation between the location of a particular mutation in the channel protein and the type of epilepsy (Milligan et al., 2014). Our patient cohort suggests otherwise, as there were unrelated patients carrying an identical mutation in *KCNT1*, despite each having been diagnosed with different types of epilepsy prior to their DNA sequencing. For example, patients 8 and 9, diagnosed with MMPSI (Ishii et al., 2013), and patient 10, an ADNFLE patient, all carried the mutant hG288S (Table 1). In addition, hR398Q, a mutation known to be associated with familial ADNFLE (Heron et al., 2012), can also lead to MMPSI, as in patient 11. A misdiagnosis of epilepsy types in these patients is highly unlikely, because MMPSI and ADNFLE are clinically distinct, and differ in age of onset, type of seizures and EEG pattern (Coppola et al., 1995; Scheffer et al., 1995). Our new finding that *KCNT1* variants are associated with multiple different epilepsies has precedence in the sodium channel *SCN1A* (Escayg et al., 2000; Lossin, 2009; Oliva et al., 2012).

Human mutations of K^+ channels that increase neuronal excitability typically reduce K^+ currents (Ryan and Ptacek, 2010). How does a gain-of-function in Slack channels lead to epileptic seizures? Slack channels contribute to the delayed outward current I_{KNa} (Budelli et al., 2009), which helps to regulate neuronal excitability and adaptability in response to high-frequency stimulation (Bhattacharjee and Kaczmarek, 2005; Brown et al., 2008; Kaczmarek,

2013; Wallen et al., 2007). Increases in I_{KNa} within a neuron, produced by enhanced cooperativity and/or by negative shifts in voltage-dependence, would therefore be expected to reduce its excitability. There are at least four conditions, however, in which increases in I_{KNa} could enhance excitability of a network. First, an increased rate of action potential repolarization due to increased K^+ current attenuates Na^+ channel inactivation and promotes high frequency firing, as is the case for Kv3 family K^+ channels (Brown and Kaczmarek, 2011). Secondly, a selective reduction in the excitability of inhibitory interneurons would enhance overall cortical excitability (Zhang et al., 2010). Thirdly, changes in action potential firing during neuronal development could produce aberrant patterns of neuronal connectivity that lead to local epileptic foci (Katz and Shatz, 1996). Finally, the very severe outcomes of mutations in Slack could occur because they alter other biochemical interactions of the channel with its cytoplasmic partners (Brown et al., 2010; Huang et al., 2013). As has been reported for some other ion channels (Deng et al., 2013; Ferron et al., 2014), the large C-terminal cytoplasmic domain of Slack interacts with the Fragile X Mental Retardation Protein (FMRP), as well as its cargo mRNAs (Brown et al., 2010). Thus, in addition to directly altering the excitability of central neurons, mutations in Slack could disrupt intracellular signaling related to FMRP and activity-dependent protein translation.

Experimental Procedures

Patients

We included 16 patients with *KCNT1* mutations in this study, including 13 reported previously. Of these, 9 and 3 total were respectively diagnosed with MMPSI (Barcia et al., 2012; Ishii et al., 2013; McTague et al., 2013) or ADNFLE (Heron et al., 2012), and one with OS (Martin et al., 2014). Three new patients were included: 2 with MMPSI and 1 with frontal epilepsy with a more severe outcome than ADNFLE for both epilepsy pharmacoresistance and cognitive outcome (Table 1). We used previously reported methods, using whole exome sequencing (MMPSI and ADNFLE) and genome sequencing (OS) approaches (Barcia et al 2012, Heron et al 2013, Martin 2014) to identify *KCNT1* mutations causative for epilepsy syndromes. Mutational analysis of *KCNT1* in these patients was carried out as described below.

Mutation analysis

KCNT1 exons were amplified by polymerase chain reaction (PCR) from DNA extracted from venous blood, using flanking intronic primers. Sequence products were run on ABI 3730 automated sequencer (Applied Biosystems) and analyzed with SeqScqpe 2.5 (Applied Biosystem). Site-directed mutagenesis of the rat Slack-B construct was performed as already described (Barcia et al., 2012), and mutations were confirmed by DNA sequencing. *Electrophysiological characterization in* Xenopus oocytes: KCNT1 channels were characterized in oocytes injected with 10 ng of cRNA, as described previously (Barcia et al., 2012). For whole-oocyte two-electrode voltage clamp experiments, electrodes were filled with 3 M KCl and had resistances of 0.1–1.0 MΩ. The bath solution, MND-96, contained (in mM) 88 NaCl, 1 KCl, 2 $MgCl_2$, 1.8 $CaCl_2$, 5 glucose, 5 HEPES, 5 sodium pyruvate and 50 μg/μl gentamicin (Gibco), pH 7.4. For measurements of channel activation, oocytes were

depolarized by 400-ms pulses from a holding potential of −80 mV to test voltages between −80 mV and +60 mV in 20-mV increments every 5 s.

For patch clamp recording, cRNA-injected oocytes were manually devitellinized in a hypertonic solution containing (in mM) 220 Na^+ aspartate, 10 KCl, 2 $MgCl_2$ and 10 HEPES. On-cell patch recordings were performed using a symmetrical high K^+ internal pipette and bath solutions, of: (in mM) 100 K-gluconate, 40 KCl, 20 NaCl, 1 $MgCl_2$, 1 $CaCl_2$, 5 EGTA and 10 HEPES, pH 7.6. Hence, patch potentials in the text refer to expected physiological potential difference across the membrane (i.e. −80 mV represents hyperpolarization). Although our analysis was carried out using stable cell-attached patches, we routinely observed that enhanced cooperativity persisted after excision of the patches from cells. Excised patches were not analyzed, however, because of the potential rundown of channel activity that is known to occur for many channels following excision.

Protein analysis

Crude membrane fractions were isolated from oocytes (Bröer, 2003). Protein samples(40 μg), separated on a 4-15% gradient SDS gel, and transferred to nitrocellulose paper, were probed overnight at 4°C with primary antibody as indicated: we used chicken anti-Slack IgY (1:5000 (Bhattacharjee et al., 2002)), rabbit anti-Na^+/K^+ ATPase IgG (1:1000; #3010, Cell Signaling), and horse anti-mouse (#PI-2000, Vector Labs) or goat anti-rabbit (#7074, Cell Signaling) HRP-conjugated secondary antibodies. Densitometry values from developed and imaged blots were determined using ImageJ.

Statistical analysis

Data recording and analysis were performed using pClamp (Molecular Devices), Origin (Microsoft) and Prism (GraphPad). The average±SEM values are plotted. Where 2 groups were compared, 2-tailed student's t-test was performed to compare statistical significance; where 3 or more groups were compared, 1-way ANOVA test was performed, followed by Bonferroni's post-hoc test, unless indicated otherwise.

Acknowledgements

This work was supported in part by the US National Institutes of Health (NIH) grants HD067517 to LKK and 5R25NS079193 to IHQ.

References

Barcia G, Fleming MR, Deligniere A, Gazula VR, Brown MR, Langouet M, Chen H, Kronengold J, Abhyankar A, Cilio R, et al. De novo gain-of-function KCNT1 channel mutations cause malignant migrating partial seizures of infancy. Nat Genet. 2012; 44:1255–1259. [PubMed: 23086397]

Bhattacharjee A, Gan L, Kaczmarek LK. Localization of the Slack potassium channel in the rat central nervous system. The Journal of Comparative Neurology. 2002; 454:241–254. [PubMed: 12442315]

Bhattacharjee A, Kaczmarek L. For K+ channels, Na+ is the new Ca2+ Trends Neurosci. 2005; 28:422–428. [PubMed: 15979166]

Bröer S. Xenopus laevis Oocytes. Methods Mol Biol. 2003; 227:245–258. [PubMed: 12824652]

Brown M, Kronengold J, Gazula V, Chen Y, Strumbos J, Sigworth F, Navaratnam D, Kaczmarek L. Fragile X mental retardation protein controls gating of the sodium-activated potassium channel Slack. Nat Neurosci. 2010; 13:819–821. [PubMed: 20512134]

Brown M, Kronengold J, Gazula V, Spilianakis C, Flavell R, von Hehn C, Bhattacharjee A, Kaczmarek L. Amino-termini isoforms of the Slack K+ channel, regulated by alternative promoters, differentially modulate rhythmic firing and adaptation. J Physiol. 2008; 586:5161–5179. [PubMed: 18787033]

Brown MR, Kaczmarek LK. Potassium channel modulation and auditory processing. Hearing Res. 2011; 279:32–42.

Budelli G, Hage TA, Wei A, Rojas P, Jong YJ, O'Malley K, Salkoff L. Na+-activated K+ channels express a large delayed outward current in neurons during normal physiology. Nat Neurosci. 2009; 12:745–750. [PubMed: 19412167]

Chen H, Kronengold J, Yan Y, Gazula V, Brown M, Ma L, Ferreira G, Yang Y, Bhattacharjee A, Sigworth F, et al. The N-terminal domain of Slack determines the formation and trafficking of Slick/Slack heteromeric sodium-activated potassium channels. J Neurosci. 2009; 29:5654–5665. [PubMed: 19403831]

Coppola G, Plouin P, Chiron C, Robain O, Dulac O. Migrating partial seizures in infancy: a malignant disorder with developmental arrest. Epilepsia. 1995; 36:1017–1024. [PubMed: 7555952]

Dekker JP, Yellen G. Cooperative gating between single HCN pacemaker channels. J Gen Physiol. 2006; 128:561–567. [PubMed: 17043149]

Deng PY, Rotman Z, Blundon JA, Cho Y, Cui J, Cavalli V, Zakharenko SS, Klyachko VA. FMRP regulates neurotransmitter release and synaptic information transmission by modulating action potential duration via BK channels. Neuron. 2013; 77:696–711. [PubMed: 23439122]

Ding S, Sachs F. Evidence for non-independent gating of P2X2 receptors expressed in Xenopus oocytes. BMC Neurosci. 2002; 3:17. [PubMed: 12421468]

Epi KC, Epilepsy Phenome/Genome P, Allen AS, Berkovic SF, Cossette P, Delanty N, Dlugos D, Eichler EE, Epstein MP, Glauser T, et al. De novo mutations in epileptic encephalopathies. Nature. 2013; 501:217–221. [PubMed: 23934111]

Escayg A, MacDonald BT, Meisler MH, Baulac S, Huberfeld G, An-Gourfinkel I, Brice A, LeGuern E, Moulard B, Chaigne D, et al. Mutations of SCN1A, encoding a neuronal sodium channel, in two families with GEFS+2. Nat Genet. 2000; 24:343–345. [PubMed: 10742094]

Ferron L, Nieto-Rostro M, Cassidy JS, Dolphin AC. Fragile X mental retardation protein controls synaptic vesicle exocytosis by modulating N-type calcium channel density. Nature Comm. 2014; 5:3628.

Heron SE, Smith KR, Bahlo M, Nobili L, Kahana E, Licchetta L, Oliver KL, Mazarib A, Afawi Z, Korczyn A, et al. Missense mutations in the sodium-gated potassium channel gene KCNT1 cause severe autosomal dominant nocturnal frontal lobe epilepsy. Nat Genet. 2012; 44:1188–1190. [PubMed: 23086396]

Horio Y, Hibino H, Inanobe A, Yamada M, Ishii M, Tada Y, Satoh E, Hata Y, Takai Y, Kurachi Y. Clustering and enhanced activity of an inwardly rectifying potassium channel, Kir4.1, by an anchoring protein, PSD-95/SAP90. J Biol Chem. 1997; 272:12885–12888. [PubMed: 9148889]

Huang F, Wang X, Ostertag EM, Nuwal T, Huang B, Jan YN, Basbaum AI, Jan LY. TMEM16C facilitates Na(+)-activated K+ currents in rat sensory neurons and regulates pain processing. Nat Neurosci. 2013; 16:1284–1290. [PubMed: 23872594]

Ishii A, Shioda M, Okumura A, Kidokoro H, Sakauchi M, Shimada S, Shimizu T, Osawa M, Hirose S, Yamamoto T. A recurrent KCNT1 mutation in two sporadic cases with malignant migrating partial seizures in infancy. Gene. 2013

Joiner WJ, Tang MD, Wang LY, Dworetzky SI, Boissard CG, Gan L, Gribkoff VK, Kaczmarek LK. Formation of intermediate-conductance calcium-activated potassium channels by interaction of Slack and Slo subunits. Nat Neurosci. 1998; 1:462–469. [PubMed: 10196543]

Kaczmarek LK. Slack, Slick and Sodium-Activated Potassium Channels. ISRN Neurosci. 2013:ii, 354262.

Katz LC, Shatz CJ. Synaptic activity and the construction of cortical circuits. Science. 1996; 274:1133–1138. [PubMed: 8895456]

Krouse ME, Wine JJ. Evidence that CFTR channels can regulate the open duration of other CFTR channels: cooperativity. J Membr Biol. 2001; 182:223–232. [PubMed: 11547345]

Laver DR, O'Neill ER, Lamb GD. Luminal Ca2+-regulated Mg2+ inhibition of skeletal RyRs reconstituted as isolated channels or coupled clusters. J Gen Physiol. 2004; 124:741–758. [PubMed: 15545399]

Lossin C. A catalog of SCN1A variants. Brain Dev. 2009; 31:114–130. [PubMed: 18804930]

Martin HC, Kim GE, Pagnamenta AT, Murakami Y, Carvill GL, Meyer E, Copley RR, Rimmer A, Barcia G, Fleming MR, et al. Clinical whole-genome sequencing in severe early-onset epilepsy reveals new genes and improves molecular diagnosis. Hum Mol Gen. 2014; 23:3200–3211. [PubMed: 24463883]

Marx SO, Gaburjakova J, Gaburjakova M, Henrikson C, Ondrias K, Marks AR. Coupled gating between cardiac calcium release channels (ryanodine receptors). Circ Res. 2001; 88:1151–1158. [PubMed: 11397781]

Marx SO, Ondrias K, Marks AR. Coupled gating between individual skeletal muscle Ca2+ release channels (ryanodine receptors). Science. 1998; 281:818–821. [PubMed: 9694652]

McTague A, Appleton R, Avula S, Cross JH, King MD, Jacques TS, Bhate S, Cronin A, Curran A, Desurkar A, et al. Migrating partial seizures of infancy: expansion of the electroclinical, radiological and pathological disease spectrum. Brain. 2013; 136:1578–1591. [PubMed: 23599387]

Milligan CJ, Li M, Gazina EV, Heron SE, Nair U, Trager C, Reid CA, Venkat A, Younkin DP, Dlugos DJ, et al. KCNT1 gain of function in 2 epilepsy phenotypes is reversed by quinidine. Annals of Neurol. 2014; 75:581–590.

Molina ML, Barrera FN, Fernandez AM, Poveda JA, Renart ML, Encinar JA, Riquelme G, Gonzalez-Ros JM. Clustering and coupled gating modulate the activity in KcsA, a potassium channel model. J Biol Chem. 2006; 281:18837–18848. [PubMed: 16670090]

Naundorf B, Wolf F, Volgushev M. Unique features of action potential initiation in cortical neurons. Nature. 2006; 440:1060–1063. [PubMed: 16625198]

Navedo MF, Cheng EP, Yuan C, Votaw S, Molkentin JD, Scott JD, Santana LF. Increased coupled gating of L-type Ca2+ channels during hypertension and Timothy syndrome. Circ Res. 2010; 106:748–756. [PubMed: 20110531]

Oliva M, Berkovic SF, Petrou S. Sodium channels and the neurobiology of epilepsy. Epilepsia. 2012; 53(11):1849–59. [PubMed: 22905747]

Ryan DP, Ptacek LJ. Episodic neurological channelopathies. Neuron. 2010; 68:282–292. [PubMed: 20955935]

Scheffer IE, Bhatia KP, Lopes-Cendes I, Fish DR, Marsden CD, Andermann E, Andermann F, Desbiens R, Keene D, Cendes F, et al. Autosomal dominant nocturnal frontal lobe epilepsy. A distinctive clinical disorder. Brain. 1995; 118(Pt 1):61–73. [PubMed: 7895015]

Vacher H, Trimmer JS. Trafficking mechanisms underlying neuronal voltage-gated ion channel localization at the axon initial segment. Epilepsia. 2012; 53(Suppl 9):21–31. [PubMed: 23216576]

Vaithianathan T, Manivannan K, Kleene R, Bahr BA, Dey MP, Dityatev A, Suppiramaniam V. Single channel recordings from synaptosomal AMPA receptors. Cell Biochem and Biophys. 2005; 42:75–85. [PubMed: 15673930]

Vanderver A, Simons C, Schmidt JL, Pearl PL, Bloom M, Lavenstein B, Miller D, Grimmond SM, Taft RJ. Identification of a novel de novo p.Phe932Ile KCNT1 mutation in a patient with leukoencephalopathy and severe epilepsy. Pediatr Neurol. 2014; 50:112–114. [PubMed: 24120652]

Wallen P, Robertson B, Cangiano L, Low P, Bhattacharjee A, Kaczmarek LK, Grillner S. Sodium-dependent potassium channels of a Slack-like subtype contribute to the slow afterhyperpolarization in lamprey spinal neurons. J Physiol. 2007; 585:75–90. [PubMed: 17884929]

Yuan A, Santi C, Wei A, Wang Z, Pollak K, Nonet M, Kaczmarek L, Crowder C, Salkoff L. The sodium-activated potassium channel is encoded by a member of the Slo gene family. Neuron. 2003; 37:765–773. [PubMed: 12628167]

Yuan A, Leonetti MD, Pico AR, Hsiung Y, MacKinnon R. Structure of the human BK channel Ca2+-activation apparatus at 3.0 A resolution. Science. 2010; 329:182–186. [PubMed: 20508092]

Zhang Z, Rosenhouse-Dantsker A, Tang QY, Noskov S, Logothetis DE. The RCK2 domain uses a coordination site present in Kir channels to confer sodium sensitivity to Slo2.2 channels. J Neurosci. 2010; 30:7554–7562. [PubMed: 20519529]

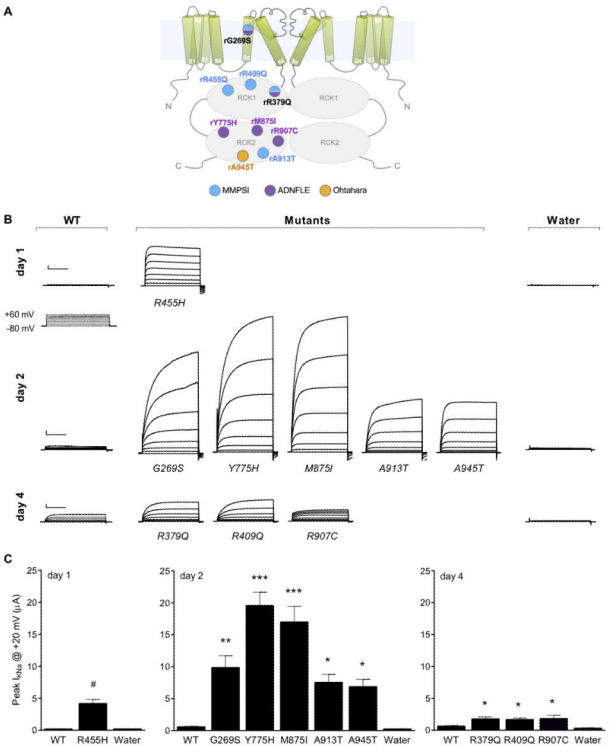

Figure 1.

Slack currents are increased by mutations that produce epilepsy. A. Diagram of two subunits of a Slack channel with the point mutations described in this study. Numbering refers to the rat Slack sequence. Positions of the mutations within the C-terminal "gating ring," containing two RCK domains (Regulators of Conductance for K, RCK1 and RCK2), are based on low resolution X-ray structure (Yuan et al. 2010). B. Voltage-clamp protocol and representative current traces showing that peak current amplitude (I_{KNa}) is significantly increased in all mutants, compared to the wild-type (WT) channel. *Xenopus* oocytes injected with cRNA encoding WT or mutant channels, or injected with water alone, were tested using a two-electrode voltage clamp on days 1, 2 or 4 following injection. Scale bars 1 μA, 200 ms. C. Bar graphs quantifying the increase in mean peak current amplitude at +20 mV for all mutant channels compared to WT Slack (mean±SEM, #p<0.01 against WT, 2-tailed student's t-test, n=5; *p<0.05, **p<0.01, ***p<0.001 against WT, 1-way ANOVA with Tukey's post-hoc test, n=6-9 for all conditions).

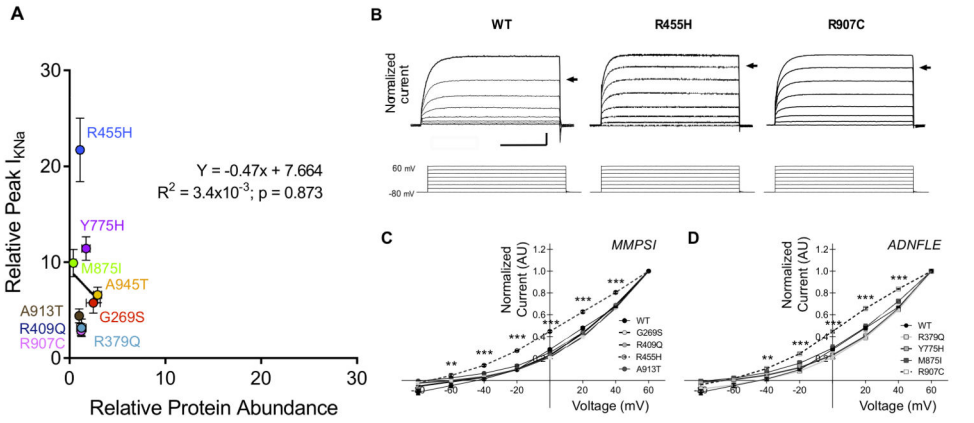

Figure 2.

A. Channel protein expression is not altered by mutations. A plot of relative increase in peak I_{KNa} changes vs levels of Slack protein determined by densitometry of western blots of membrane fractions from oocytes homogenized immediately after the voltage-clamp experiments. A non-significant best-of-fit (solid line) shows no relationship that can account for the increases in current. B. Voltage-dependence of channel activation is shifted leftward in the R455H and R907C mutants. Representative traces for WT, R455H and R907C mutants, normalized to their peak I_{KNa} at +60 mV. The shift in voltage-dependence is made evident by the position of arrows lined up to the responses to test pulses at +40 mV. C and D. Mean peak I_{KNa} at each of the command voltages shown as an I/V plot for MMPSI (C) and ADNFLE (D) mutants. Current amplitudes were normalized to the peak I_{KNa} at +60 mV in all cases. In the R455H mutant, the Increase in relative channel activity was seen at voltages ≥ −60 mV and −40 mV for R455H (C) and R907C (D), respectively (*p<0.05, **p<0.01, ***p<0.001 against WT, 2-way ANOVA with Bonferroni's post-hoc test, n = 5-10 for all points).

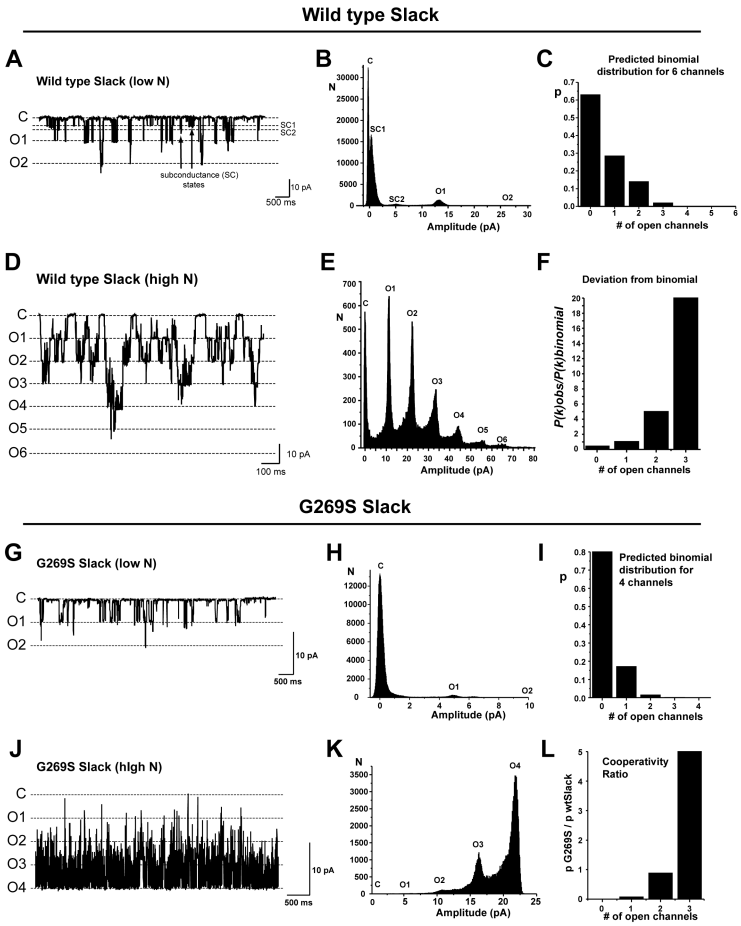

Figure 3.

Single channel recordings of WT and G269S Slack in *Xenopus* oocytes. A. Representative on-cell single channel “low N” traces recorded at −80 mV, and the corresponding all points amplitude histogram (B). The C, O1 and O2 labels represent the closed and various open states. SC1 and SC2 indicate the two prominent subconductance states. C. Binomial distribution for 6 channels, based on the single channel opening probability *P*o in low N patches (mean of 8 low N patches). D. Representative on-cell high N patch recorded at −80 mV. E. All points amplitude histogram of currents from panel D. Experimental data show the increased frequency of multiple channel openings and dramatic reduction in dwell time in the fully closed state compared to the expected binomial distribution in C. F. Deviation from binomial distribution. The plot shows the ratio of the observed *P*o at each level, $P(k)_{obs}$, compared to the predicted distribution obtained from the binomial distribution (C), P(*k*)*binomial*, for the first three levels. The ratios continue to increase with successive *k* for 4, 5 and 6 channels (not shown). G. Representative on-cell, single channel low N trace of G269S channels at −80 mV, and the corresponding all points amplitude histogram (H), representing 2 minutes of recording. I. Binomial distribution for 4 channels based on the mean single channel Po in low N patches (n=4 low N patches). J. Representative on-cell high N patch containing four G269S channels. K. The corresponding all points amplitude histogram, showing a dramatically increased frequency of multiple channel openings compared to the expected binomial distribution (I). L. Cooperativity Ratio, comparing

$P(k)_{obs}$ for G269S vs. WT Slack. The ratios were calculated from the means of 4 and 5 high N patches for G269S and WT Slack, respectively. The ratios show a deviation from the expected value of 1 for each successive *k*, demonstrating increased positive cooperativity relative to WT Slack. The ratio for 4 open channels is 53 (not shown).

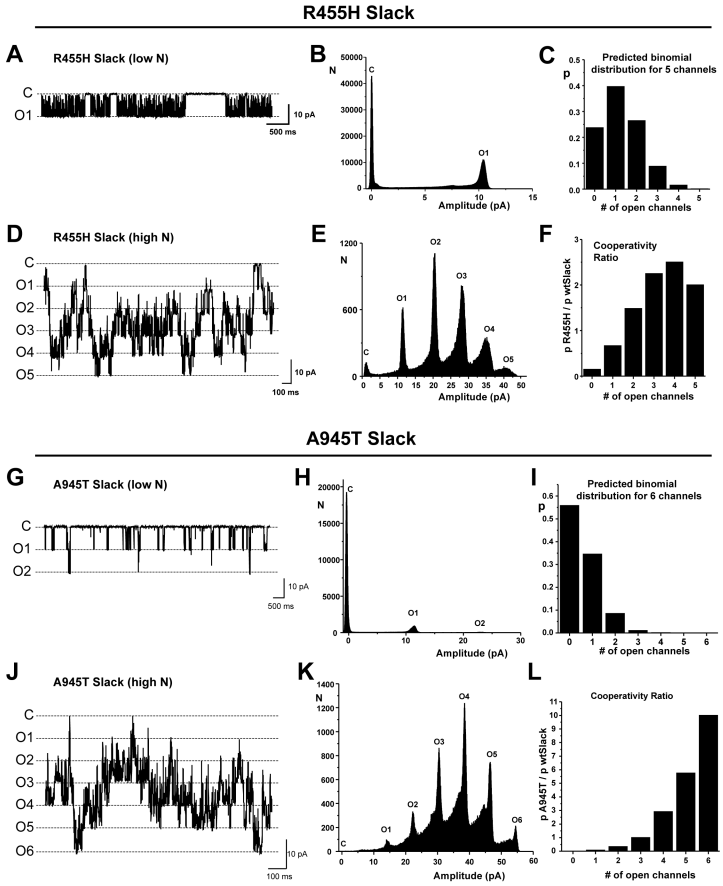

Figure 4.

Single channel recordings of Slack mutants R455H and A945T in *Xenopus* oocytes. A. Representative on-cell single channel trace recorded at −80 mV from a patch expressing Slack R455H, and the corresponding all points amplitude histogram **(**B). C. Binomial distribution for 5 R455H channels, based on the mean single channel *P*o from 4 low N R455H patches. Representative high N trace (D) and all points amplitude histogram (E) from a patch containing 5 Slack R455H channels. F. Cooperativity Ratios (comparing $P(k)_{obs}$ for R455H vs. WT Slack) were calculated from the means of 3 and 5 high N patches for G455R and WT Slack, respectively. The ratio shows a significant deviation from the expected value of 1 for all 5 channel openings. Representative low N recording (G) and corresponding all points amplitude histogram (H) from a patch containing A945T channels −80 mV. I. Binomial distribution for 6 channels, based on the mean single channel *P*o in low N A945T patches (n=5 low N patches). Representative high N recording (J) and corresponding all points amplitude histogram (K) from patches containing 6 A945T channels. L. The Cooperativity Ratio, as calculated from the means of 3 and 5 high N patches for A945T and WT Slack, respectively.

Table 1

Clinical and Biophysical Characteristics of Human Mutant Slack Channels

Patient #	Mutation	Protein		Epilepsy type	Age at seizure onset (type)	Pharmaco resistance	Intellectual Delay	Micro-cephaly	Previous reference	Peak current	Protein expression	I/V	Conductance (i)
		Human	Rat										
1	c.1283G>A	R428Q	R409Q	MMPSI	2m	Y	Y	Y	Barcia et al., 2012	↑ 3-fold	NC*	NC*	Fewer SC**, same i#
2	c.1283G>A	R428Q	R409Q	MMPSI	1d	Y	Y	Y	Barcia et al., 2012				
3	c.1283G>A	R428Q	R409Q	MMPSI	2h	Y	Y	Y	Barcia et al., 2012				
4	c.2800G>A	A934T	A913T	MMPSI	1m	Y	Y	Y	Barcia et al., 2012	↑ 4-fold	NC	NC	Fewer SC, same i
5	c.2800G>A	A934T	A913T	MMPSI	2w	Y	Y	Y	McTague et al., 2013				
6	c.2800G>A	A934T	A913T	MMPSI	2.5m (focal motor)	Y	Y	Y	--				
7	c.1421G>A	R474H	R455H	MMPSI	2w	Y	Y	Y	Barcia et al., 2012	↑ 22-fold	NC	Leftward shift	Fewer SC, same i
8	c.862G>A	G288S	G269S	MMPSI	2m (focal motor)	Y	Y	Y	Ishii et al., 2013	↑ 6-fold	NC	NC	Fewer SC, 50% i
9	c.862G>A	G288S	G269S	MMPSI	2m (focal motor with autonomic signs)	Y	Y	Y	Ishii et al., 2013				
10	c.862G>A	G288S	G269S	ADNFLE	3y	Y	Y	N	--				
11	c.1193G>A	R398Q	R379Q	MMPSI	10d (focal motor)	Y	Y	NK	--	↑ 3-fold	NC	NC	Same i
12 (Fam.C)	c.1193G>A	R398Q	R379Q	ADNFLE	8.5y±6.4	0/4	2/4	NK	Heron et al., 2012				
13 (Fam.B)	c.2386T>C	Y796H	Y775H	ADNFLE	5.5y±2.1	2/4	2/4	NK	Heron et al., 2012	↑ 11-fold	NC	NC	Same i
14 (Fam.D)	c.2688G>A	M896I	M875I	ADNFLE	9y	1/1	1/1	NK	Heron et al., 2012	↑ 10-fold	Reduced 2 fold	NC	80% i
15 (Fam.A)	c.2782C>T	R928C	R907C	ADNFLE	4.6y±5.9	5/6	3/6	NK	Heron et al., 2012	↑ 3-fold	NC	Leftward shift	Same i
16	c.2896G>A	A966T	R945T	OS	1d	Y	Y	NK	Martin et al., 2014	↑ 13-fold	NC	NC	Fewer SC, same i

* No change (NC)

** indicates few occurrences of subconductance (SC) states

# indicates relative change in unitary conductance (i)